Accepted Manuscript

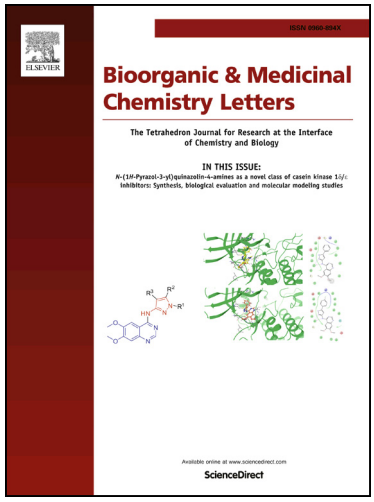

Design, synthesis of novel furan appended benzothiazepine derivatives and *in vitro* biological evaluation as potent VRV-PL-8a and H^+/K^+ ATPase inhibitors

Devirammanahalli Mahadevaswamy Lokeshwari, Nanjappagowda Dharmappa Rekha, Bharath Srinivasan, Hamse Kameshwar Vivek, Ajay Kumar Kariyappa

PII: S0960-894X(17)30547-4
DOI: http://dx.doi.org/10.1016/j.bmcl.2017.05.059
Reference: BMCL 25004

To appear in: *Bioorganic & Medicinal Chemistry Letters*

Received Date: 10 March 2017
Revised Date: 18 April 2017
Accepted Date: 19 May 2017

Please cite this article as: Lokeshwari, D.M., Rekha, N.D., Srinivasan, B., Vivek, H.K., Kariyappa, A.K., Design, synthesis of novel furan appended benzothiazepine derivatives and *in vitro* biological evaluation as potent VRV-PL-8a and H^+/K^+ ATPase inhibitors, *Bioorganic & Medicinal Chemistry Letters* (2017), doi: http://dx.doi.org/10.1016/j.bmcl.2017.05.059

Design, synthesis of novel furan appended benzothiazepine derivatives and *in vitro* biological evaluation as potent VRV-PL-8a and H^+/K^+ ATPase inhibitors

Devirammanahalli Mahadevaswamy Lokeshwari,[a] Nanjappagowda Dharmappa Rekha,[b] Bharath Srinivasan,[c] Hamse Kameshwar Vivek,[d] Ajay Kumar Kariyappa[a]*

[a]*Department of Chemistry, Yuvaraja College, University of Mysore, Mysuru. India.*

[b]*Department of Biotechnology, JSS College for Arts, Commerce & Science, Mysuru. India.*

[c]*Center for the Study of Systems Biology, School of Biology, Georgia Institute of Technology, Atlanta, Georgia 30332, USA.*

[d]*Sri Ram Chem, R & D Centre, Plot No 31, JCK Industrial Park, Belagola Industrial Area, Mysuru- 570006, India.*

Abstract

A series of new of furan derivatised [1, 4] benzothiazepine analogues were synthesized starting from 1-(furan-2-yl)ethanone. 1-(furan-2-yl)ethanone was converted into chalcones by its reaction with various aromatic aldehydes, then were reacted with 2-aminobenzenethiol in acidic conditions to obtain the title compounds in good yields. The synthesized new compounds were characterized by ^{1}H NMR, ^{13}C NMR, Mass spectral studies and elemental analyses. All the new compounds were evaluated for their *in vitro* VRV-PL-8a and H^+/K^+ ATPase inhibitor properties. Preliminary studies revealed that, some molecules amongst the designed series showed promising VRV-PL-8a and H^+/K^+ ATPase inhibitor properties. Further, rigid body docking studies were performed to understand possible docking sites of the molecules on the target proteins and the mode of binding. This finding presents a promising series of lead molecules that can serve as prototypes for the treatment of inflammatory related disorder that can mitigate the ulcer inducing side effect shown by other NSAIDs.

Keywords: Antidiabetic, anti-inflammatory, benzothiazepines, chalcones, 1-(furan-2-yl)ethanone.

The heterocyclic nucleus of thiazepine is present in a number of bioactive molecules, and is recognized as a key building block for the synthesis of small-molecules with potential pharmaceutical activities.[1] The broad spectrum of clinical applications and commercial success associated with benzothiazepine derivatives have placed them as important molecules in the field of medicinal chemistry.[2] Various protocols have been developed for the synthesis of benzothiazepines in literature. To mention two representative examples: the reaction of acid amides with phosphoryl chloride furnishes 2,3-dihydro-l,4-benzothiazepine[3] and the one-pot reaction between 2-aminobenzo[*d*]isothiazol-3-one and alkyl propiolates in the presence of triphenylphosphine produces 1,4-benzothiazepines.[4]

Further, molecules possessing benzothiazepine skeleton have exhibited high biological profiles.[5] These classes of compounds have been known to show anti-arrhythmic, angiogenic, central nervous system activities,[6] antimicrobial,[7] antioxidant,[8] anti-inflammatory, analgesics, antitumor, and anticonvulsant properties.[9] 1,4-Benzothiazepine derivatives also show interesting neuroprotective activity in addition to their demonstrated blockade of the mitochondrial sodium/calcium exchanger.[10] The chemical modification of heterocyclic systems by devising a new protocol for design of new compounds with high pharmacological profile is always a challenge for the medicinal chemist. We herein report the synthesis of functionalized 1,4-benzothiazepine derivatives and *in vitro* screening results for their VRV-PL-8a and H^+/K^+ ATPase inhibitor properties.

The strategy adopted for the synthesis of the target compounds, **3**(**a-h**), is depicted in **Fig. 1**. The intermediate chalcones, **3**(**a-h**), were synthesized by the Claisen-Schmidt condensation reaction of 1-(furan-2-yl)ethanone, **1,** and aromatic aldehydes, **2**(**a-h**), in the presence of potassium hydroxide in methyl alcohol. Then, the chalcones, **3**(**a-h**), were

transformed in to target molecules **5**(**a-h**) by their reaction with 2-aminobenzenethiol, **4,** and concentrated hydrochloric acid (4-6 drops) in methyl alcohol under reflux conditions.

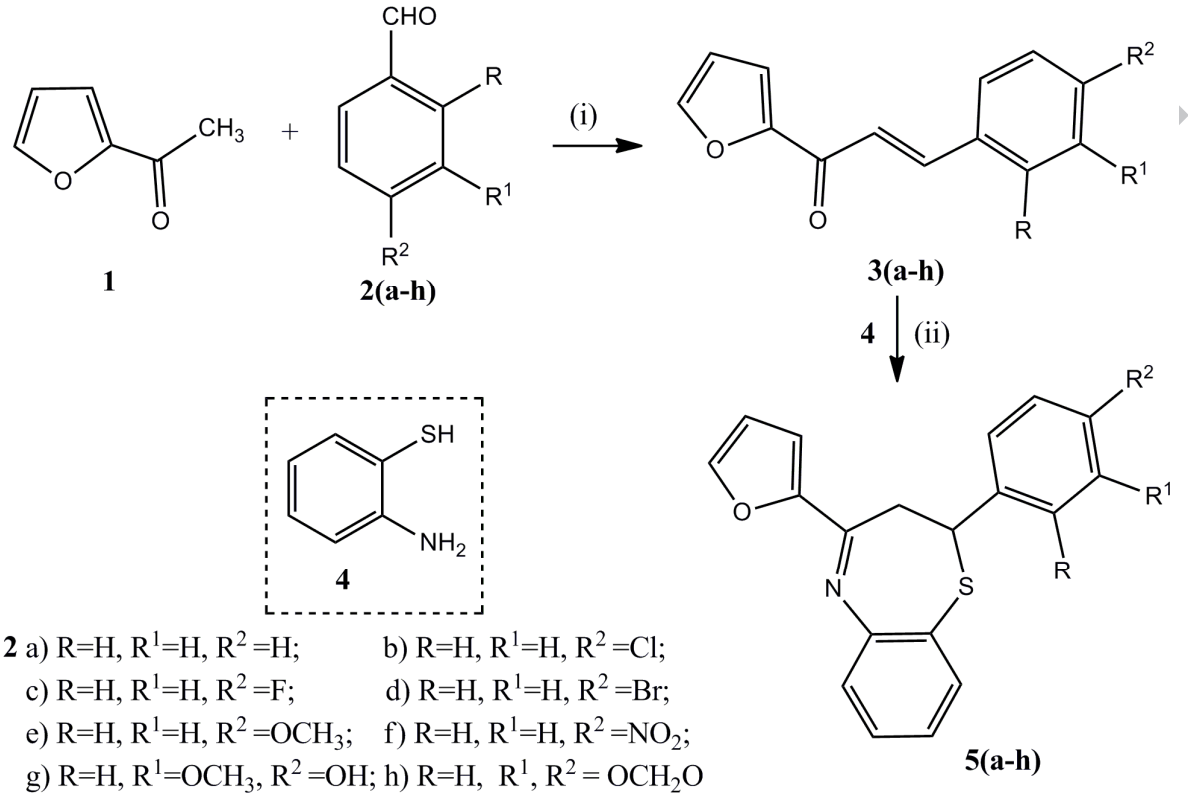

1 **2(a-h)**

2 a) R=H, R^1=H, R^2 =H; b) R=H, R^1=H, R^2 =Cl;
c) R=H, R^1=H, R^2 =F; d) R=H, R^1=H, R^2 =Br;
e) R=H, R^1=H, R^2 =OCH_3; f) R=H, R^1=H, R^2 =NO_2;
g) R=H, R^1=OCH_3, R^2 =OH; h) R=H, R^1, R^2 = OCH_2O

Reagents and condition: (i) EtOH/KOH, rt, 2-3 h; (ii) MeOH/HCl, 160 ^oC, 4 h

Fig. 1. Schematic diagram for the synthesis of benzothiazepines, **5**(**a-h**)

The resultant structures of the synthesized compounds **3**(**a-h**) and **5**(**a-h**) were confirmed by ^1H NMR, ^{13}C NMR, Mass spectral studies and CHN analyses. In ^1H NMR spectrum, compound **3b** showed two doublets for one proton each at δ 6.285 ppm and δ 6.793 ppm which were due to olefinic CH=C and C=CH protons, respectively. An array of signals observed as multiplet for seven protons at δ 7.244-8.201 ppm were due to aromatic protons. Two methylene (C-3) protons of the newly formed benzothiazepine ring in compound **5b**, exhibit typical ABX spin system, and are diastereotopic appearing as two doublet of doublets. C_3-H_a resonates with both C_3-H_b and C_2-H appearing as doublet of doublet at δ 2.923-2.985 (*J= 12.4, 24.8 Hz*) ppm and C_3-H_b resonates with both C_3-H_a and

C_2-H appearing as doublet of doublet at δ 3.214-3.259 (*J=8.0, 18.0Hz*) ppm. C_2-H coupled with both C_3-H_a and C_3-H_b and appeared as doublet of doublet at δ 5.045-5.086 (*J= 6.8, 16.4Hz*) ppm. An array of signals appearing as multiplets for eleven protons at δ 6.587-8.182 ppm were due to aromatic protons.

In ^{13}C NMR spectrum, compound **3b** showed signals at δ 121.41, 144.63 and 170.44 ppm due to olefinic CH=, =CH, and C=O carbons, respectively. Aromatic carbons showed the signals in the region δ 112.10-153.86 ppm. For compound **5b**, the signals due to C-2, C-3 and C-4 carbons of the newly formed thiazepine ring appeared at δ 34.54, 25.76 and 158.32 ppm, respectively. Aromatic carbons showed the signals in the region δ 110.32-153.09 ppm. Para substitution effect caused the two carbons, each at ortho and meta positions of chlorophenyl ring, to abosrb at δ 128.76 and 129.54 ppm, respectively. The NMR data of the synthesised series of compounds **3**(**a-h**) and **5**(**a-h**) are tabulated in **Table 1**.

Table 1. NMR spectral data of compounds **3**(**a-h**) and **5**(**a-h**).

	^{1}H NMR ($CDCl_3$): δ ppm	^{13}C NMR ($CDCl_3$): δ ppm
3a	6.282 (d, 1H, *J=6.9Hz*), 6.834 (d, 1H, *J=7.6Hz*), 7.241-8.128 (m, 8H).	111.33, 114.85, 121.28, 127.66, 128.34, 128.88, 134.20, 144.40, 148.55, 154.20, 170.20 (C=O).
3b	6.285 (d, 1H, *J=7.1Hz*), 6.793 (d, 1H, *J=9.0Hz*), 7.244-8.201 (m, 7H).	112.10, 115.28, 121.41, 128.26, 128.82, 133.10, 133.77, 144.63, 147.88, 153.86, 170.44 (C=O).
3c	6.406 (d, 1H, *J=6.6Hz*), 6.903 (d, 1H, *J=7.8Hz*), 7.122-8.040 (m, 7H).	112.50, 115.62, 116.80, 121.88, 129.96, 131.49, 144.84, 148.46, 151.30, 161.30, 170.77 (C=O).
3d	6.451 (d, 1H, *J=6.0Hz*), 6.945 (d, 1H, *J=8.7Hz*), 7.230-8.304 (m, 7H).	112.38, 115.74, 121.60, 123.50, 129.56, 132.84, 133.90, 145.04, 146.55, 151.33, 170.16 (C=O).
3e	3.840 (s, 3H), 6.286 (d, 1H, *J=7.3Hz*),	111.98, 114.50, 116.42, 121.44, 127.14,

	6.794 (d, 1H, *J=9.5Hz*), 7.024-8.004 (m, 7H).	131.08, 145.10, 146.90, 152.22, 158.20, 169.80 (C=O).
3f	6.451 (d, 1H, *J=6.2Hz*), 6.963 (d, 1H, *J=7.8Hz*), 7.280-8.344 (m, 7H).	112.14, 116.63, 121.50, 124.46, 129.60, 140.81, 146.06, 146.63, 147.75, 152.80, 169.95 (C=O).
3g	3.866 (s, 3H, *J=7.5Hz*), 5.807 (s, 1H), 6.389 (d, 1H, *J=10.1Hz*), 6.908 (d, 1H), 7.025-7.972 (m, 6H).	110.10, 112.40, 116.56, 117.77, 120.18, 123.30, 127.10, 128.34, 145.32, 147.12, 147.96, 148.26, 154.19, 169.80 (C=O).
3h	6.122 (s, 2H, *J=7.3Hz*), 6.344 (d, 1H, *J=8.9Hz*), 6.866 (d, 1H), 7.186-8.064 (m, 6H).	100.12, 105.24, 109.34, 113.42, 117.44, 121.20, 122.65, 126.88, 143.33, 147.28, 148.78, 152.26, 169.16 (C=O).
5a	2.892-2.960 (dd, 1H, *J= 12.0, 27.2Hz*), 3.240-3.286 (dd, 1H, *J= 8.3, 18.4Hz*), 5.060-5.109 (dd, 1H, *J= 6.9, 19.6Hz*), 6.620-8.126 (m, 12H).	26.87 (C-3), 36.89 (C-2), 113.80, 122.29, 124.09, 124.16, 125.64, 125.94, 127.12, 128.97, 130.34, 135.03, 145.70, 147.37, 150.55, 151.85, 152.42, 159.14 (C-4).
5b	2.923-2.985 (dd, 1H, *J= 12.4, 24.8Hz*), 3.214-3.259 (dd, 1H, *J= 8.0, 18.0Hz*), 5.045-5.086 (dd, 1H, *J= 6.8, 16.4Hz*), 6.587-8.182 (m, 11H).	25.76 (C-3), 34.54 (C-2), 110.32, 122.29, 125.21, 125.66, 126.21, 127.04, 128.76, 129.54, 132.76, 139.54, 145.65, 150.85, 151.32, 153.09, 158.32 (C-4).
5c	2.980-3.038 (dd, 1H, *J= 12.0, 23.2Hz*), 3.288-3.331 (dd, 1H, *J= 8.1, 17.2Hz*), 5.080-5.124 (dd, 1H, *J= 6.9, 17.6Hz*), 6.68-8.14 (m, 11H).	26.26 (C-3), 36.89 (C-2), 113.32, 120.65, 123.21, 126.98, 128.43, 130.94, 131.06, 133.86, 135.76, 138.54, 142.41, 148.05, 151.43, 153.21, 158.76 (C-4).
5d	2.881-2.943 (dd, 1H, *J= 12.5, 24.8Hz*), 3.260-3.308 (dd, 1H, *J= 9.1, 19.2Hz*), 5.100-5.146 (dd, 1H, *J= 8.1, 18.4Hz*), 6.66-8.18 (m, 11H).	28.32 (C-3), 34.21 (C-2), 110.21, 119.65, 120.54, 123.65, 126.32, 130.14, 131.46, 132.21, 135.11, 137.32, 141.34, 146.76, 150.21, 152.33, 156.54 (C-4).
5e	2.955-3.010 (dd, 1H, *J= 12.9, 22.0Hz*), 3.260-3.305 (dd, 1H, *J= 8.1, 18.0Hz*), 3.625 (s, 3H), 5.060-5.108 (dd, 1H, *J= 6.4, 19.2Hz*), 6.682-8.183 (m, 11H).	27.62 (C-3), 32.65 (C-2), 55.41, 111.43, 115.21, 119.33, 120.65, 122.55, 125.17, 129.21, 132.21, 134.65, 136.21, 140.31, 143.43, 149.21, 152.87, 156.88 (C-4).
5f	2.864-2.928 (dd, 1H, *J= 12.7,*	27.76 (C-3), 32.54 (C-2), 111.40, 115.25,

	26.6Hz), 3.165-3.202 (dd, 1H, *J= 8.6, 15.2Hz*), 3.72 (s, 3H), 5.162-5.198 (dd, 1H, *J= 7.2, 14.4Hz*), 6.730-8.452 (m, 11H).	119.20, 121.60, 122.51, 125.33, 129.56, 132.06, 134.30, 136.20, 140.50, 143.88, 149.10, 152.80, 157.12 (C-4).
5g	2.771-2.829 (dd, 1H, *J= 12.0, 23.2Hz*), 3.240-3.283 (dd, 1H, *J= 8.0, 17.2Hz*), 3.61 (s, 3H), 5.091-5.137 (dd, 1H, *J= 7.3, 18.4Hz*), 6.745-8.223 (m, 11H).	27.76 (C-3), 32.68 (C-2), 59.46, 111.67, 115.34, 119.86, 120.88, 122.66, 125.78, 129.30, 132.23, 134.87, 136.25, 140.65, 143.65, 149.67, 152.89, 156.89 (C-4).
5h	2.920-2.976 (dd, 1H, *J= 11.7, 22.4Hz*), 3.091-3.135 (dd, 1H, *J= 8.5, 17.6Hz*), 3.69 (s, 3H), 5.180-5.226 (dd, 1H, *J= 6.0, 18.4Hz*), 6.690-8.229 (m, 11H).	27.89 (C-3), 32.87 (C-2), 59.67, 111.87, 115.56, 119.72, 120.77, 122.78, 125.38, 129.37, 132.45, 134.86, 136.45, 140.68, 143.76, 149.98, 152.88, 156.88 (C-4).

In mass spectra, compounds **3g** and **5g** showed base peaks at m/z 244.09 and 351.03 respectively, corresponding to their molecular massess. Except, the compounds with chloro and bromo substitutions, all compounds amongest the series **3**(**a-h**) and **5**(**a-h**) showed the base peaks corresponding to their molecular masses. Compounds **3b** and **5b,** having chloro substitutions, and **3d** and **5d,** having bromo substitutions, showed base peaks at their respective molecular masses and M+2 peaks due to isotopes ^{37}Cl, ^{81}Br with relative abundances of 34%, 34%, 98%, 97.2% respectively. All compounds showed satisfactory elemental analyses data.

Inflammation is a complex immunological cascade driven by several different factors and can be initiated by manifold cues including, but not limited to, pathogen invasion, tissue damage due to oxidative challenge etc. COX-2 is an important player in bringing about inflammation. Primarily during tissue damage, the first enzyme to get activated is sPLA2, which drives the substrate for COX-2. Inhibition of sPLA2 will result in substrate depletion for COX-2, thereby bringing down the inflammation, as there will be no pro-inflammatory

and inflammatory Prostaglandins (PG). In this context, we assessed the inhibitory potential of the newly synthesized benzothiazepines to inhibit sPLA2, rather than COX-2.[11]

As a prototype to test our findings, $sPLA_2$ (VRV-PL-8a) from *V. russelli* venom was employed instead of the human homologue. The protein was purified to homogeneity by reported procedure,[12] and estimated by Lowry's method.[13] *In vitro* inhibition of $sPLA_2$ (VRV-PL-8a) by the synthesized benzothiazepine derivatives, **5**(**a-h**) was assayed according to reported procedure.[14] Further, indirect hemolytic activity of the synthesized benzothiazepine derivatives, **5**(**a-h**), was assayed by reported method.[15] The series of benzothiazepine derivatives **5(a-h)** were assessed for $sPLA_2$ inhibition studies and the results are tabulated in Table 2.

Furthermore, the H^+/K^+-ATPase (pig stomach mucosal membrane) inhibition activity of the synthesized benzothiazepine derivatives, **5**(**a-h**) was also determined as described by W B Im.[16] The gastric H^+/K^+-ATPase, together with Na^+/K^+-ATPase and Ca^{2+}-ATPase, is a member of the P-type ATPase. The ion pump is an essential electrogenic pump maintaining potential difference across the intracellular and extracellular compartments in a cellular matrix by retaining low sodium and high potassium intracellularly. These proteins engage in a common catalytic cycle with ion translocation coupled to phosphorylation and dephosphorylation of a conserved aspartate residue.[17] Some of them belong to the Haloacid dehalogenase family of enzyme with a conserved DXDXV/T motif, with the second aspartate in the motif critical for the formation of the phosphoenzyme intermediate.[18] The assay was carried out by initiating the ATPase reaction by the addition of the substrate (ATP), carried out at 37 °C for 15 mins and stopped with 1.0 mL ice cold 20 % TCA. The liberated inorganic phosphate from ATP was estimated by Fiske Subbarow's method.[19] The assessed H+/K+ ATPase activity is reported in Table 2.

Table 2. Neutralization of VRV-PL-8a ($sPLA_2$) and H^+/K^+ ATPase by compounds **5**(**a-h**)[#]

Test compound	sPLA$_2$ IC$_{50}$ (µM) ± SEM	H+/K+ ATPase IC$_{50}$ (µM) ± SEM
5a	12.014 ± 0.110	8.014 ± 0.076
5b	19.287 ± 0.162	5.277 ± 0.051
5c	25.192 ± 0.205	5.099 ± 0.051
5d	24.142 ± 0.190	2.112 ± 0.021
5e*	**11.014** ± 0.101	**1.989** ± 0.020
5f	56.882 ± 0.507	3.732 ± 0.037
5g	43.410 ± 0.394	4.390 ± 0.042
5h	25.128 ± 0.221	5.143 ± 0.050

*5e denotes the potent ligand; #the experiments were performed in quadruplicates (n=4) and the results are reported as mean of the values ± SEM.

The tested benzothiazepine derivatives, **5(a-h)** inhibited sPLA$_2$ in dose depended manner with an IC$_{50}$ value ranging from 11.01 to 56.88 µM which are computed and analyzed using sigmoidal 4PL curve fit. Among the tested compounds, **5e** showed significant inhibition against VRV-PL-8a with IC$_{50}$ value of 11.01µM (**Fig. 2**), when compared to other structurally related molecules. *In-situ* indirect hemolytic activity of VRV-PL-8a in presence of compounds **5e** was evaluated using egg yolk and packed erythrocytes as substrate. VRV-PL-8a alone exhibited 96 ± 2.0% hemolysis of erythrocyte (positive control) when compared with pure water (100% lysis). VRV-PL-8a incubated with **5e** (0-100µM) respectively for 60 min at 37°C, inhibited hemolysis in a dose dependent manner with an IC$_{50}$ of 21.23 ± 2.1 µM as estimated by non-linear fit (**Fig. 3**).

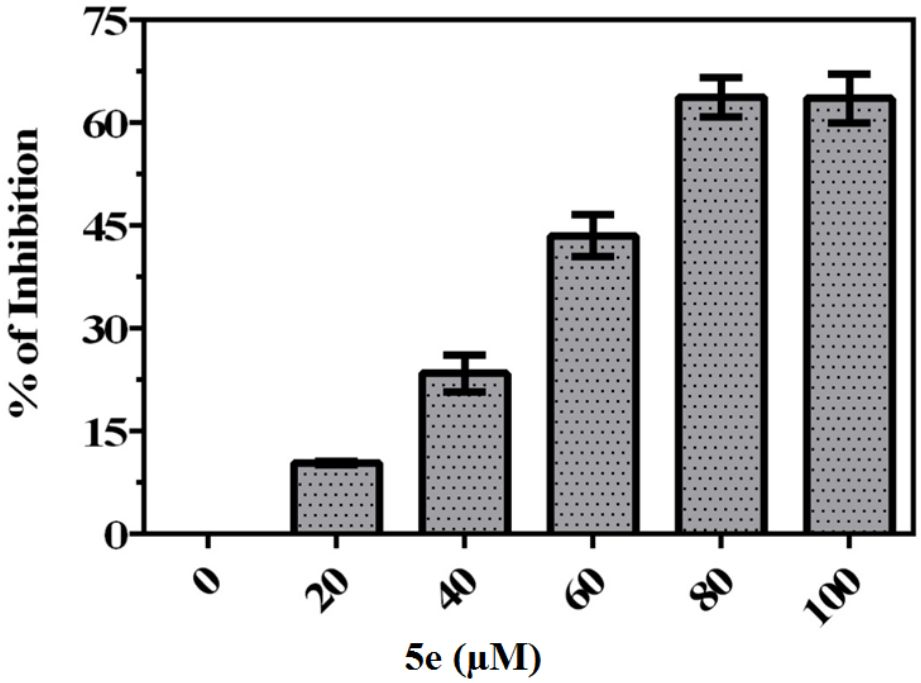

Fig. 2. Neutralization of indirect haemolytic activity of VRV-PL-8a by compound **5e**. Values represent means ±SEM (n = 4).

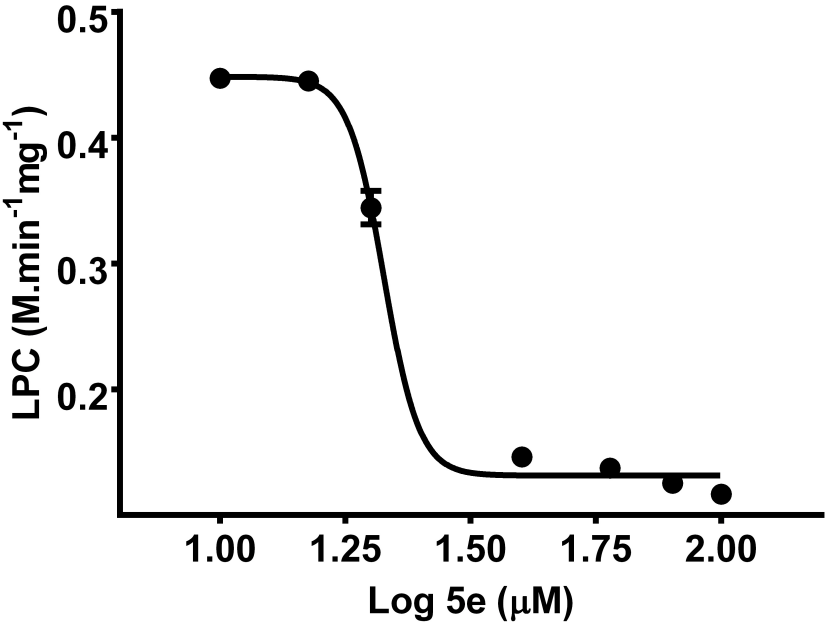

Fig. 3. Dose-response curves-showing the effect of **5e** on VRV-PL-8a. IC_{50} was calculated using sigmoidal four parameter logistic fit (4PL) plot. Values represent means ±SEM (n = 4).

To understand the mechanism of action of inhibition, we studied the effect of substrate and calcium concentrations on VRV-PL-8a enzyme inhibition by **5e**. We examined its inhibition as a function of calcium and substrate concentrations. **5e** at its IC_{50} concentration (11.01µM) and with varying calcium concentration 0-12mM, showed no change in $sPLA_2$ activity neither did it change the extent of inhibition of **5e, Fig. S1(a)**. This indicates to possible non-competition of compound **5e** with the calcium binding site or the active site on the VRV-PL- 8a enzyme. Thus, it can be surmised that inhibition of $sPLA_2$ by **5e** is independent of calcium concentration and is not brought about by chelating calcium ions required for the enzyme activity. Effect of **5e** (11.01µM) on varying DMPC substrate concentration (0-400µM) was evaluated. $sPLA_2$ activity increased with increased substrate concentration **Fig. S1(b)**; suggesting that **5e** does not compete with substrate binding site on VRV-PL-8a. In presence of **5e,** only 51% enzyme activities was observed at maximum substrate concentration of 400 µM. GII PLA_2 has a conserved active site within a hydrophobic channel lined by invariant hydrophobic residues. The active site residues His48, Asp49, Tyr52 and Asp99 are directly connected to the channel.[20] His48 is known to play a major role in catalysis by facilitating the formation of hydrogen bond between Asp99 and Asp49 via water molecule that is part of the catalytic network. It is known that, any structural perturbations in His48, at the N-terminal α-helix of $sPLA_2$, plays an important role in both membrane binding of the enzyme and substrate binding to the catalytic site that reduces the binding affinity of the enzyme-substrate complex.[21]

In order to determine the possible binding modes for compound **5e,** molecular docking studies were performed for ligands **5(a-h).** The structure of the protein from *Daboia russelii* (PDB ID: 1SXK) was employed for docking studies. Analysis of the interaction mode for the lower energy docking pose among the ensemble indicated that compound **5a** interacted with Phe5, His48 and Tyr52 by π-π stacking (**Fig. 4**). Whereas, in case of **5e**,

Lys69, Trp31 and His48 interacted with the small molecule by π-π stacking (**Fig. 5**). Importantly, binding of ligand **5e** near the α-helical random coil clearly suggests that it had interaction with His48, which resides near the random coil.[22]

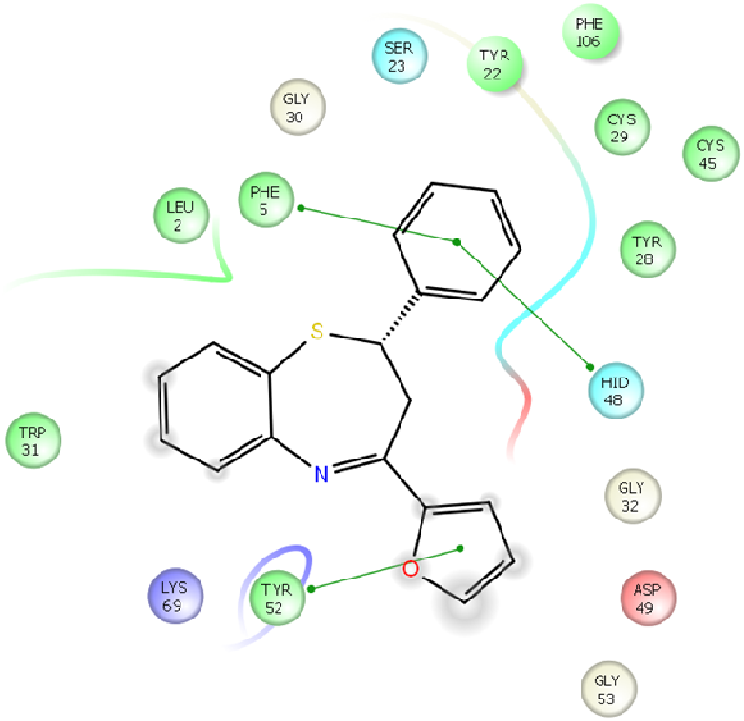

Fig. 4. *In silico* analysis of VRV-PL-8a with **5a,** Molecular docking studies showed an interacting map of **5a** with VRV-PL-8a showing molecular interaction.

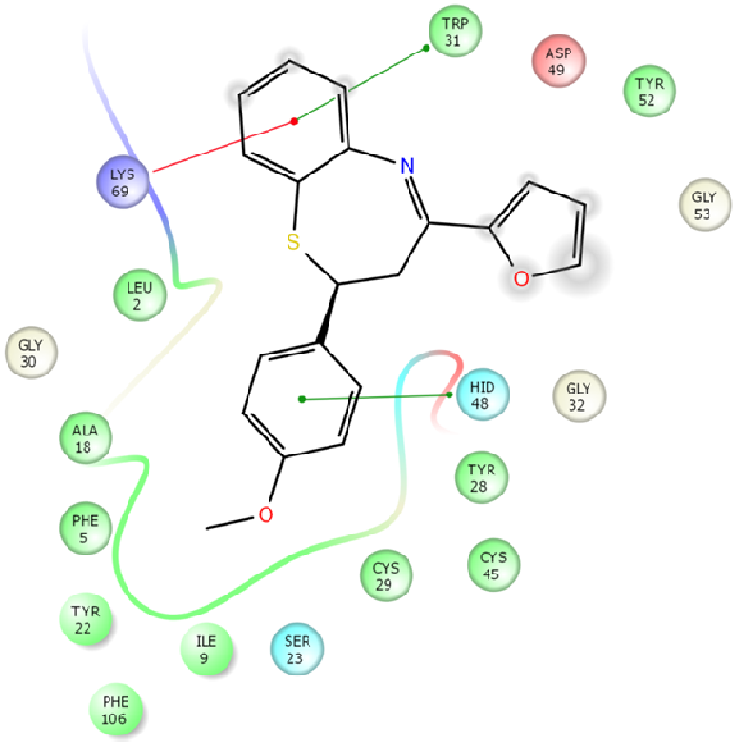

Fig. 5. *In silico* analysis of VRV-PL-8a with **5e,** Molecular docking studies showed an interacting map of **5e** with VRV-PL-8a showing molecular interaction.

Likewise, to rationalize the inhibition seen for Na+/K+ ATPase and o gain insights into the possible binding modes, rigid-body docking studies of the compounds was carried out with the receptor structure. Crystal structure of Na^+/K^+-ATPase from *Squalus acanthias* (Spiny Dogfish) (PDB ID: 2ZXE) was used for molecular docking studies as a prototype instead of the structure of the protein from human for ease of target structure preparation. Molecular docking studies showed an interacting map of Na^+/K^+-ATPase (**Fig. 6** and **Fig. 7**) with compound **5a** and **5e** respectively. Based on XP glide score, **5e** showed a promising scoring function, when compared to other structurally related compounds (**Table 3**). Additionally, the low E model value indicated that the binding affinity between protein and ligand is energetically favorable.[23]

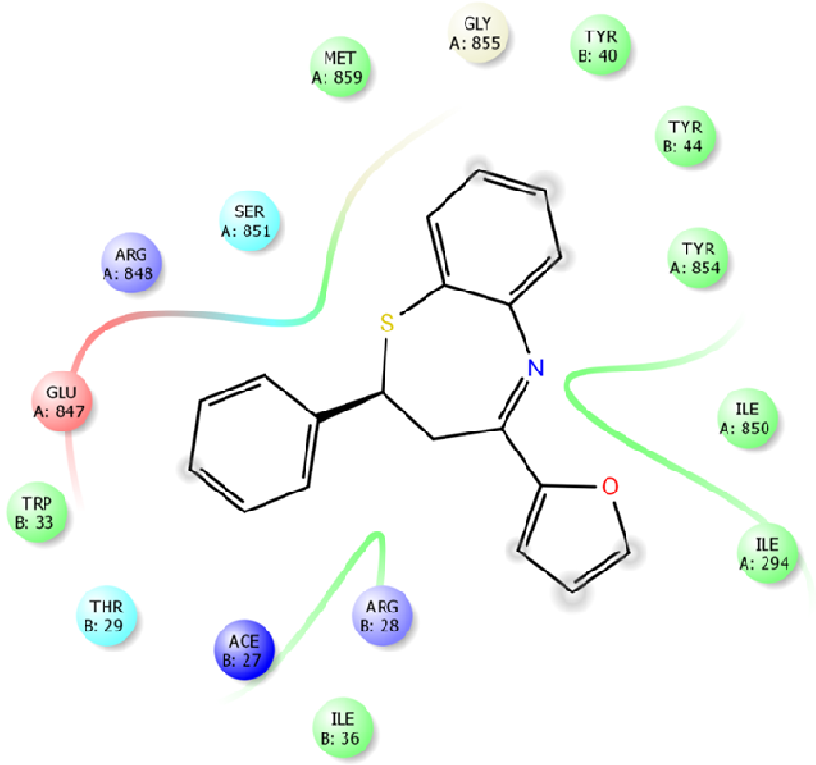

Fig. 6. *In silico* analysis of Na^+/K^+-ATPase pump with **5a,** Molecular docking studies showed an interacting map of **5a** with Na^+/K^+-ATPase showing molecular interaction.

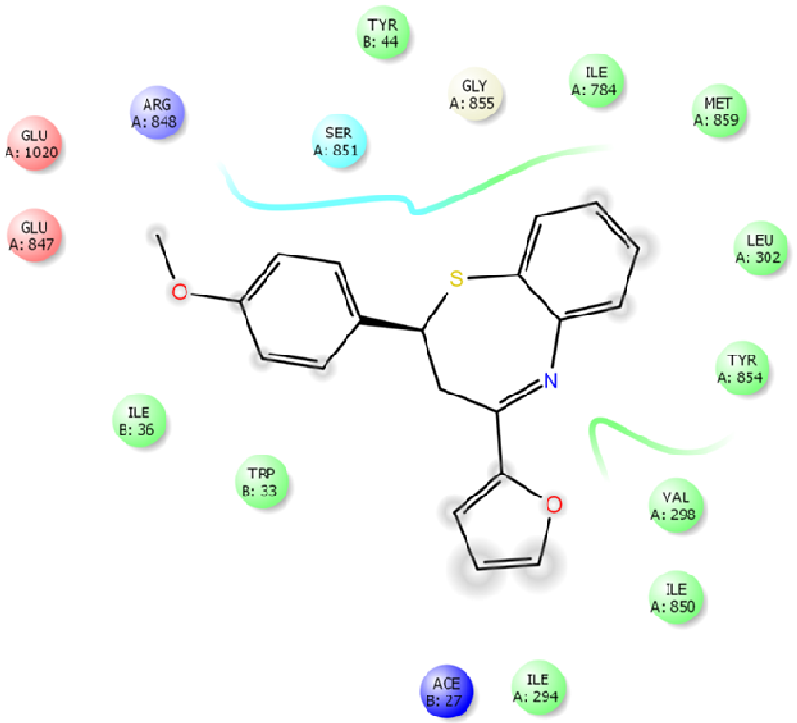

Fig. 7. *In silico* analysis of Na^+/K^+-ATPase pump with **5e,** Molecular docking studies showed an interacting map of **5e** with Na^+/K^+-ATPase showing molecular interaction.

Pharmacodynamics parameters play an important role in determining the success of a lead candidate for further therapeutic development. ADME descriptors were computed for the various synthesized compounds. ADME descriptors simulation suggests that **5e** is better drug molecule which falls within the range of 95% of drugs (**Table S1**).

Table 3: Molecular docking scores of all synthesized compounds against VRV-PL-8a and Na+/K+ ATPase as obtained through Glide docking.

Ligand	1SXK				2ZXE			
	RMSD OPLS-2005	Docking score	Glide gscore	Glide emodel	RMSD OPLS-2005	Docking score	Glide gscore	Glide emodel
5a	0.002	-5.08	-5.09	-51.82	0.003	-5.42	-5.43	-39.34
5b	0.036	-4.96	-4.97	-46.18	0.012	-5.42	-5.44	-40.01
5c	0.003	-4.59	-4.60	-46.51	0.002	-5.46	-5.48	-43.18
5d	0.038	-4.89	-4.91	-51.14	0.036	-5.67	-5.69	-42.94
5e	**0.012**	**-5.10**	**-5.11**	**-49.15**	**0.032**	**-6.02**	**-6.04**	**-46.82**

5f	0.002	-3.99	-4.00	-43.49	0.002	-5.53	-5.54	-38.75
5g	0.001	-4.11	-4.12	-48.21	0.007	-5.51	-5.53	-42.10
5h	0.003	-4.84	-4.85	-46.30	0.003	-5.43	-5.45	-39.33

Recent studies show that over 50% of patients consuming known NSAIDs like Fenoprofen, Diclofenac, Ibuprofen, etc., undergo major damage to their small intestine.[24,25] This necessitates that better small-molecules with lesser side-effects and better pharmacological properties are discovered. This study is an attempt, among many others, that attempts to discover novel small molecules that have both NSAID and gastric ATPase inhibition properties.

In summary, in order to develop anti-inflammatory and antiulcer agents, we have synthesized series of bioactive benzothiazepines and evaluated them for anti-inflammatory and ATPase inhibitory activities. Compounds inhibiting $sPLA_2$ have been implicated as potential therapeutic agents in the treatment of inflammatory disorders. Hence, we targeted the primary enzyme ($sPLA_2$), which drives the inflammatory cascade. Use of NSAIDs causes' gastric ulcer, hence anti-inflammatory and ulcer activities are closely related in order to bring down inflammation. Compound **5e** showed both better anti-inflammatory as well as ATPase inhibitory activities. Thus, **5e** could be promising drug in treating inflammatory related disorder that can mitigate the ulcer inducing side effect shown by other NSAIDs.

Acknowledgements

The authors are grateful to the IOE Instrumentation Facility, Vijnana Bhavana, University of Mysore, for recording spectra of the synthesized compounds.

References

1. Shi, F.; Zeng, X, -N,; Cao, X, -D.; Zhang, S.; Jiang, B.; Zheng, W. -F.; Tu, S. -J. *Bioorg. Med. Chem. Lett.* **2012**, *22,* 743.
2. McCauley, M. D.; Wehrens, X. H. T. *Acta Pharma. Sinica*. **2011**, *32,* 749.

3. Janoss, Z. -G.; Ernatha, A. B.; Gnes, K. -C.; Odor, D. L. *Can. J. Chem*. **1987**, *65,* 175.
4. Incerti, M.; Acquotti, D.; Sandor, P.; Vicini, P. *Tetrahedron*. **2009**, *65*, 7487.
5. Christopher, B. W. P.; Christopher, S. P. M. *Tetrahedron Lett*. **2011**, *52,* 1490.
6. El-Bayouki, A. M. K. *J. Sulfur Chem*. **2011**, *32,* 623.
7. Raghavendra, K. R.; Ajay Kumar, K.; Shashikanth, S. *Int. J. Pharm. Pharm. Sci.* **2014**, *6(5),* 90.
8. Renuka, N.; Pavithra, G.; Ajay Kumar, K. *Der Pharma Chemica* **2014**, *6(1),* 482.
9. Bakavoli, M.; Rahimizadeh, M.; Raissi, H.; Beyzaei, H.; Tajabadi, J. *Monatshefte für Chemie* **2008**, *139,* 1211.
10. Francisco, J. M. S.; Rocío, L. -C.; Ana, J. M. -O.; Laura, G. -L.; Jose, C. F.-M.; Raquel, L. -A.; María, F. C. -A.; Cristobal de los. R. *ACS Chem. Neurosci*. **2015**, *6,* 1626.
11. Kameshwar, V. H.; Kumar, J. R.; Babu, S.; Priya, S.; Nanjunda Swamy. *Mol. Cell Biochem.* doi:10.1007/s11010-016-2888-6.
12. Kasturi, S.; Gowda, T.V. *Toxicon* **1989,** *27,* 229.
13. Lowry, O. H.; Rosebrough, N. J.; Farr, A. L.; Randall, R.J. *J. Biol. Chem.* **1951**, *193,* 265.
14. Vivek, H. K; Swamy, S. G.; Priya, B. S.; Sethi, G.; Rangappa, K. S.; Nanjunda Swamy, S. *Ana. Biochem.* **2014**, *461,* 27.
15. Boman, H. G.; Kalletta, U. *Bio. Biophys. Acta*. **1957,** *24,* 619.
16. Im, W. B.; Sih, J. C.; Blakeman, D. P.; McGrath, J. P. *J. Bio. Chem*. **1985**, *260,* 4591.
17. Kim, C. G.; Watts, J. A.; Watts, A. *J. Med. Chem*. **2005**, *48*, 7145.
18. Srinivasan, B; Nagappa LK; Shukla A; Balaram H, **2015** *Exp Parasitology* 151, 56.
19. Fiske, C. H; Subbarow, Y. *J. Biolog. Chem*. **1925**, *66,* 375.
20. Kini, R. M. *Toxicon*. **2003**, *42,* 827.
21. Yu, L.; Dennis, E. A. *Proc. Nat. Acad. Sci*. **1991**, *88,* 9325.

22. Hosadurga, K.K.; Hamse, K.V.; Hanumantharayappa, B.; Shobith, R.; Krishna, C.B.; Lewis, H. M.; Julian, E. F.; Priya, B. S.; Basappa; Nanjunda S. S; Andreas, B.; Rangappa, K. S. *RSC Adv*. **2015**, *5,* 89797.

23. Husain, A.; Ajmal, M. *Acta Pharm.* **2009**, *59,* 223.

24. Sharma, S. P.; Kumar, N.; Dudhe, R. *Der Pharma Chemica* **2010**, *2,* 253.

25. Higuchi, K.; Umegaki, E.; Watanabe, T.; Yoda, Y.; Morita, E.; Murano, M.; Tokioka, S.; Arakawa, T. *J. Gastroenterol.* **2009**, *44,* 879.